

ON THE FLOW CURVE PEAK FORECASTING VIA ARTIFICIAL NEURAL NETWORKS

¹Petr OPĚLA, ¹Ivo SCHINDLER, ¹Stanislav RUSZ, ¹Michal SAUER

¹VSB - Technical University of Ostrava, Ostrava, Czech Republic, EU, petr.opela@vsb.cz

<https://doi.org/10.37904/metal.2022.4466>

Abstract

Artificial neural networks (ANN) embody the wide family of various brain-inspired approaches finding their utilization at the solution of many up-to-date issues, e.g., voice, picture and video processing and recognition or regression analysis. The ANN-based regression analysis is able to provide a functional relationship between the high number of predictors and high number of outcomes. This ANN ability has been in the frame of the submitted research applied to offer an alternative methodism for the forecasting of hot flow curve global maximum coordinates under a wide range of thermomechanical circumstances. The research is aimed to evaluate three types of ANN - a Multi-Layer Perceptron (MLP), Radial Basis Neural Network (RBNN) and Generalized Regression Neural Network (GRNN). The results have showed that considering the description of both peak point coordinates simultaneously, the RBNN two-outputs model offered the best performance from the point of view of achieved accuracy, forecasting ability and even feasible computing time.

Keywords: Hot flow curve peak, regression analysis, multi-layer perceptron, radial basis neural network, generalized regression neural network

1. INTRODUCTION

A flow stress evolution is an inevitable phenomenon accompanying any deformation procedure. Taking into account a continuous hot forming process under a constant temperature and strain rate level, the flow stress evolution is characterized by its gradual increase as the consequence of an increasing strain. However, since the effect of dynamic softening phenomena, the evoked flow stress increase is gradually retarded and subsequently terminated [1]. An achieved flow stress global maximum and its corresponding strain level (peak point coordinates) represent temperature and strain rate dependent variables, and their forecasting finds its application e.g., when modeling a flow stress evolution [2] or trying to identify the onset of a dynamic recrystallization [3]. This forecasting issue can be solved either via the well-known Zener-Hollomon parameter [4] or alternatively via a multivariate polynomial [5] approach - however always separately, i.e., one forecasting model for the peak strain and another for the peak stress [2]. The submitted research then introduces another alternative methodology which has a potential to improve the forecasting accuracy and make the description be performed via only one regression model (two-parallel-outputs model). The peak point forecasting is going to be solved via three different artificial neural network (ANN) approaches [6-8]. Specifically, via a Multi-Layer Perceptron (MLP) network [9,10], Radial Basis Neural Network (RBNN) [11,12] and Generalized Regression Neural Network (GRNN) [13]. The introduced ANN approaches will be demonstrated on a peak point dataset experimentally acquired under six deformation temperatures (1043, 1113, 1203, 1303, 1413 and 1553 K) and four strain rates (0.02, 0.2, 2 and 20 s⁻¹) - see corresponding experimental details in [14].

2. ARTIFICIAL NEURAL NETWORK REGRESSION ANALYSIS

2.1. Preparation of experimental dataset

The utilizing of an ANN regression approach always requires to divide an experimental dataset on two subsets - a training one and a forecasting one (also known as a testing subset). The training subset is directly involved

in the process of a regression model assembling and takes the biggest share of an examined dataset - ca 70 % in the current research. The rest of the studied dataset has been then applied to verify the forecasting capacity of the assembled ANNs. The specific data split is expressed in **Table 1** - where the blue and red values correspond to the training and forecasting subset, respectively. The dataset preparation phase then also consists of a necessary normalization process to ensure the smooth, fast and successful course of ANN calculations. A normalization methodism applied in the current research transforms the studied variables into dimensionless vectors always with a corresponding standard deviation equal to 1.0 - see details in [15].

Table 1 Experimental dataset and corresponding split to training (blue) and forecasting (red) subset

T (K) / $\dot{\epsilon}$ (s ⁻¹)	Peak Strain, ϵ_p (-)				Peak Stress, σ_p (MPa)			
	0.02	0.2	2	20	0.02	0.2	2	20
1553	0.10	0.16	0.26	0.34	19.70	34.81	55.88	84.60
1413	0.14	0.22	0.32	0.56	38.77	62.19	85.80	128.00
1303	0.20	0.26	0.34	0.40	66.23	96.38	135.98	172.30
1203	0.18	0.24	0.32	0.38	99.79	140.35	184.40	222.04
1113	0.26	0.38	0.36	0.40	149.97	190.19	234.00	280.40
1043	0.32	0.30	0.30	0.40	199.00	237.54	276.18	333.00

2.2. Regression analysis via multi-layer perceptron

In the current research, each examined ANN architecture mediates a functional relationship between two predictors (temperature, T (K), and strain rate, $\dot{\epsilon}$ (s⁻¹)) and two outcomes (peak strain, ϵ_p (-), and peak stress, σ_p (MPa)). The MLP-based architecture [9,10] is formed by the network of artificial neurons (computational units) arranged into layers. Each neuron provides the simple weighted sum of previous-layer neuron outputs, and such sum is in addition processed through a specific activation function (logistic sigmoid and pure line [15] as regards to the hidden layers and outcome layer, respectively). Since the introduced architecture is highly nonlinear, its regression constants (weights, W , and biases, b) had to be obtained via nonlinear least square methodism, specifically by means of the Levenberg-Marquardt iteration algorithm [16,17] with the application of the Bayesian regularization [18,19], and running under the back propagation of outcomes error [20]. The more detailed description of the utilized MLP regression approach is available e.g. in [15]. The examined MLP architecture have, in the current research, two under-change hyperparameters - the number of hidden layers and its neurons. An appropriate hyperparameter configuration has been selected on the basis of heuristic approach by examining an interval of $[1, 3] \subset \mathbb{N}$ and an interval of $[1, 20] \subset \mathbb{N}$ as regards to the number of hidden layers and neurons, respectively. An MLP network with the ideal selection of a hyperparameter configuration is schematically demonstrated in **Figure 1**.

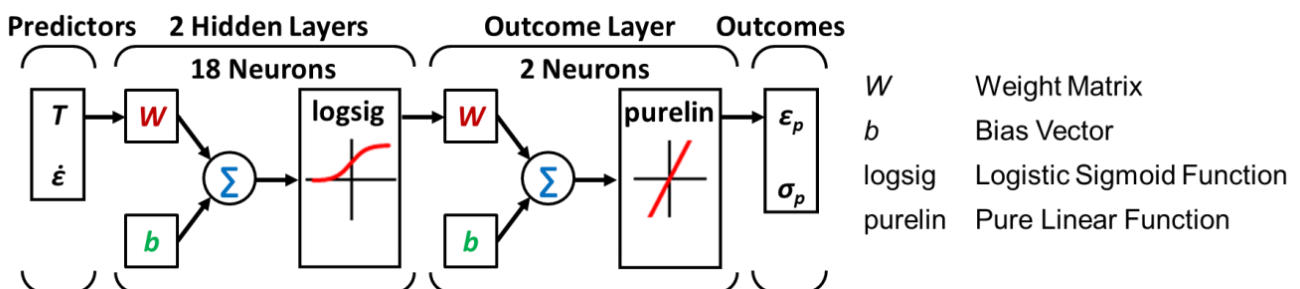


Figure 1 Block diagram of the utilized MLP architecture

2.3. Regression analysis via radial basis and generalized regression neural networks

Both the RBNN [11,12] and GRNN [13] regression techniques are based on the mapping of a low-dimensional predictor space into a high-dimensional one in order to convert a nonlinear regression issue into a linear form [21]. This is possible thanks to a radial basis hidden layer which employs the calculation of the Euclidean distances [22] between the individual datapoints of a predictor matrix and specific neuron centers (which are equal to the selected datapoints of the predictor matrix), and subsequently applies the Gaussian radial basis activation function [15,23] to return the hidden (radial basis) neuron outputs (representing a high-dimensional feature space) [15]. The response of the RBNN architecture is then simply obtained as the linear combination of high-dimensional predictor vectors. So, the regression constants (W and b) of the RBNN can be obtained via a simple linear least square method [24]. The GRNN response is, however, achieved by a slightly different way - the values of the regression constants are equal to the normalized values of corresponding outcome vectors. The more detailed description of the utilized RBNN and GRNN regression approaches is available e.g. in [15]. In contrast with the above-mentioned MLP architecture, both the RBNN and GRNN architectures have only one under-change hyperparameter - the value of a radial basis function spread. An appropriate spread has been found on the basis of a heuristic approach by examining two intervals, specifically $[0.01, 0.99] \subset \mathbb{Q}$ with a step of 0.01 and $[1, 100] \subset \mathbb{Q}$ with a step of 0.1. RBNN and GRNN architectures with the ideal selection of a spread-hyperparameter are schematically demonstrated in **Figure 2**. With respect to the RBNN, a selected spread value has a direct influence on the number of hidden layer (radial basis layer) neurons. In the case of the GRNN, however, the number of radial basis neurons is equal directly to the number of training datapoints [21].

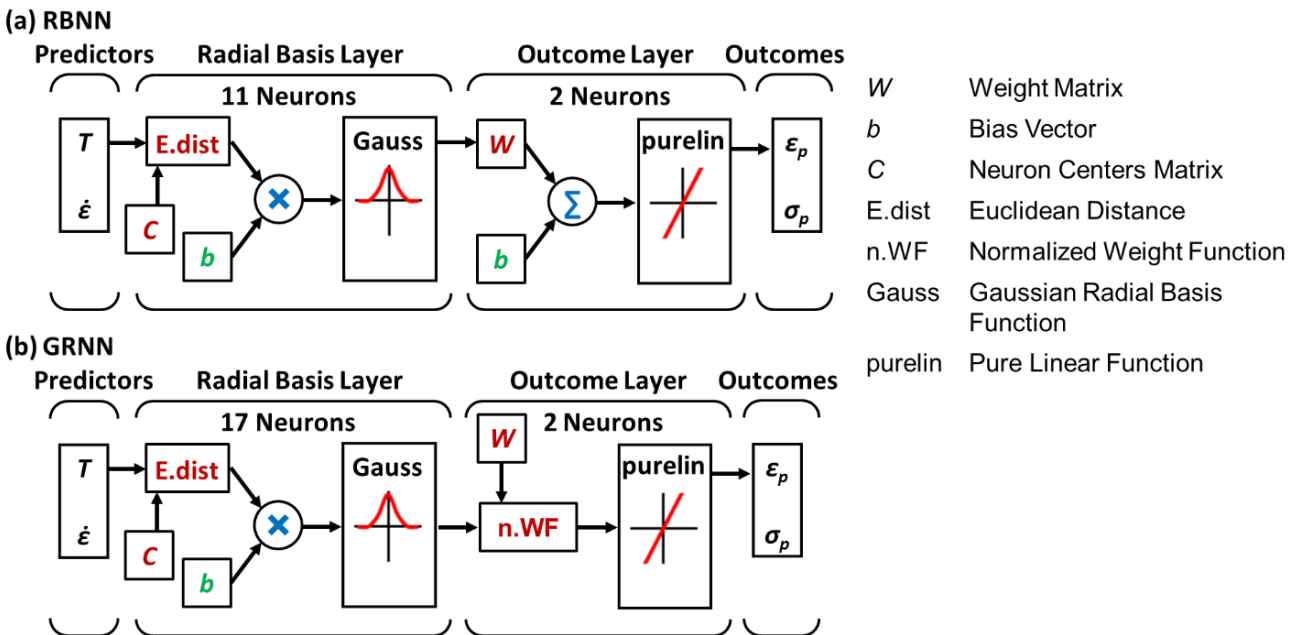


Figure 2 Block diagrams of the utilized RBNN and GRNN architectures

3. RESULTS AND DISCUSSION

The performance of the above-described ANN architectures associated with the optimized hyperparameter configurations (**Figures 1 and 2**) is graphically expressed in **Figure 3**, where the mutual comparison is mediated via the absolute errors of a network response, i.e., $\Delta_i = |E_i - C_i|$, where the variables Δ_i (-, MPa), E_i (-, MPa) and C_i (-, MPa) symbolize the absolute error, experimental (target) and calculated outcome of i -th temperature-strain rate combination, respectively, where $i = [1, 24] \subset \mathbb{N}$.

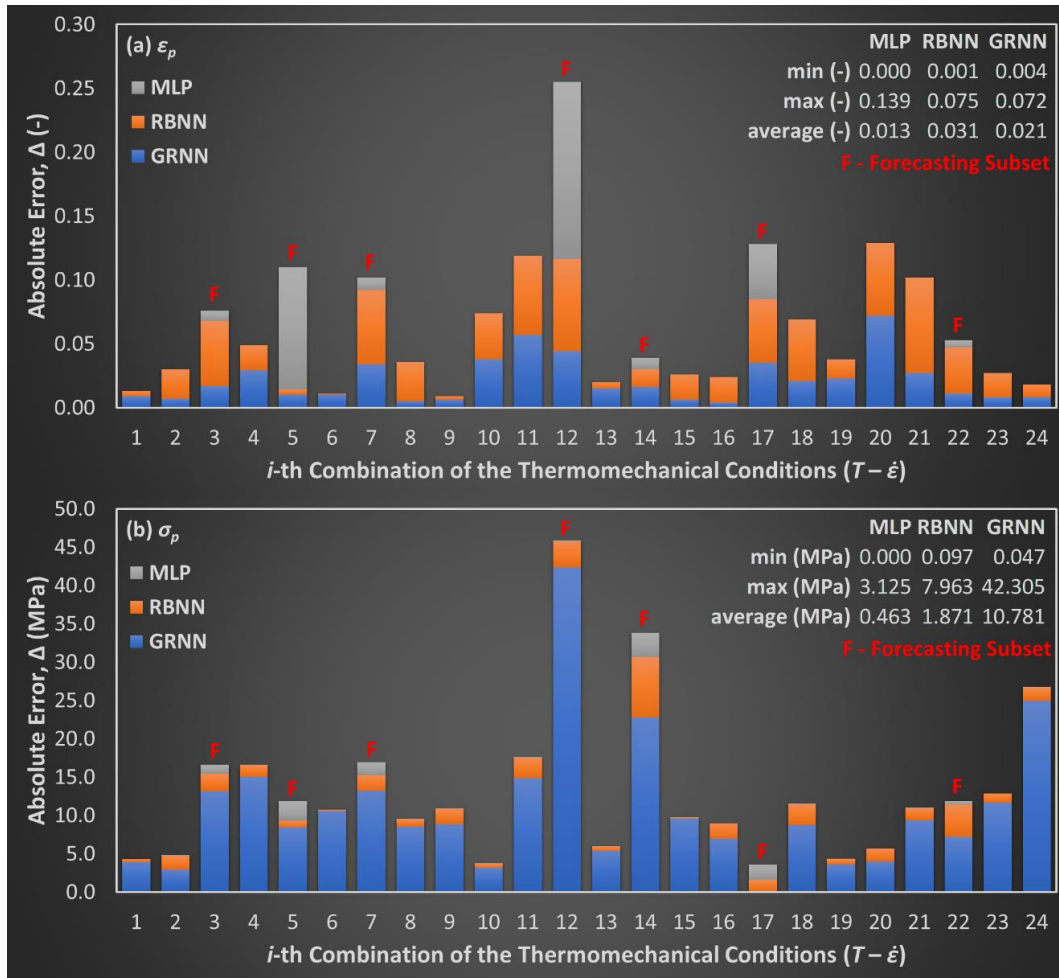


Figure 3 Performance of the examined artificial neural network approaches

Considering the peak strain calculation, it can be said that the RBNN and GRNN architectures provided the best regression response for both the training and even forecasting subset. The MLP approach then returned practically zero Δ -values when considering the subset directly utilized in the regression analysis. Higher Δ -values are then practically associated only with the forecasting subset - which indicate the occurrence of an overfitting phenomenon. Nevertheless, this does not have to immediately mean an inappropriate result; but, the obtained deviations must remain sufficiently low. However, the maximal Δ -value of the forecasting subset reaches up to 0.139 - which is unfortunately in the case of the ϵ_p -values (see **Table 1**) a considerable deviation - so, the achieved MLP forecasting performance just cannot be considered as appropriate. Taking into account the peak stress calculation, the situation is quite different. The GRNN approach is entirely inappropriate since neither the training subset nor the forecasting subset is associated with a feasible Δ -values. On the contrary, for the ϵ_p -description inappropriate MLP approach was showed to be the best choice as regards to the σ_p -description. The Δ -values higher than zero are, as in the case of the ϵ_p -description, practically associated only with the forecasting subset. However, unlike the ϵ_p -description case, the σ_p forecasting deviations are sufficiently low with the maximum of ca 3 MPa. So, the best ϵ_p -description and σ_p -description performance is associated with the GRNN and MLP methodology, respectively. Either way, this conclusion means that neither the MLP approach nor the GRNN approach was able to provide acceptable united description of both peak values only via one neural network. Nevertheless, as the **Figure 3** further indicates that the RBNN approach has been able to provide a sufficient response for both outcomes. So, despite the fact that the RBNN approach provided not entirely the best response, its performance is high enough to consider this kind of network if one wants to describe the both peak values at once. Moreover, considering the necessary computing time, the

MLP methodism was much slower since its nonlinear character. On the contrary, the RBNN and GRNN approaches were characterized by a fast calculation procedure since their above-mentioned nonlinear-to-linear transformation feature.

4. CONCLUSION

The submitted research is aimed on the assembling of a model offering the forecasting of the flow curve peak coordinates (namely, peak strain, ε_p (-), and peak stress, σ_p (MPa)) with respect to the temperature and strain rate combinations. This kind of forecasting model should thus represent the nonlinear dependency of two outcomes on two predictors. To deal with this requirement, three various Artificial Neural Network (ANN) architectures have been applied and evaluated in the sense of their forecasting ability and required computing time. A Multi-Layer Perceptron (MLP) architecture offered a highly nonlinear model which was able to precisely describe only the σ_p -outcome. A Radial Basis Neural Network (RBNN) and its modified version known as Generalized Regression Neural Network (GRNN) then offered the mapping of the low-dimensional predictor space into a high-dimensional one in which the formerly nonlinear regression task become to be linear - this led to the significant reduction of a required computing time. However, the GRNN approach was able to return a suitable network response only in the case of the ε_p -description. So, neither the MLP nor the GRNN methodism was able to provide acceptable results for both peak point coordinates when utilizing two-outputs model. Fortunately, it has been showed that the RBNN model is suitable not only from the point of view of a fast computing time but also for its ability to forecast both peak point coordinates with a suitable accuracy via only one ANN model containing two parallel outputs.

ACKNOWLEDGEMENTS

The article was created thanks to the project No. CZ.02.1.01/0.0/0.0/17_049/0008399 (ČR and EU financial funds) and the Student Grant Competitions SP2022/73 and SP2022/68 (MŠMT ČR).

REFERENCES

- [1] HOSFORD, W.F., CADDELL, R.M. *Metal Forming: Mechanics and Metallurgy*. Cambridge: Cambridge University Press, 2007.
- [2] OPĚLA, P., KAWULOK, P., SCHINDLER, I., KAWULOK, R., RUSZ, S., NAVRÁTIL, H. On the Zener-Hollomon Parameter, Multi-Layer Perceptron and Multivariate Polynomials in the Struggle for the Peak and Steady-State Description. *Metals*. 2020, vol. 10, no. 11, 1413. Available from: <https://doi.org/10.3390/met10111413>.
- [3] KAWULOK, P., OPĚLA, P., SCHINDLER, I., KAWULOK, R., RUSZ, S., SAUER, M., KONEČNÁ, K. Hot Deformation Behavior of Non-Alloyed Carbon Steels. *Materials*. 2022, vol. 15, no. 2, p. 595. Available from: <https://doi.org/10.3390/ma15020595>.
- [4] ZENER, C., HOLLON, J.H. Effect of Strain Rate upon Plastic Flow of Steel. *Journal of Applied Physics*. 1944, vol. 15, no. 1, pp. 22-32.
- [5] DESCARTES, R. *Discours de la méthode pour bien conduire sa raison, & chercher la vérité dans les sciences. Plus la dioptrique. Les météores. Et la géométrie*. [Discourse on the Method of Rightly Conducting One's Reason and of Seeking Truth in the Sciences. Plus the Dioptr, Meteors and Geometry]. Leiden: De l'imprimerie de Ian Maire, 1637.
- [6] McCULLOCH, W.S., PITTS, W.H. A Logical Calculus of the Ideas Immanent in Nervous Activity. *The bulletin of mathematical biophysics*. 1943, vol. 5, no. 4, pp. 115-133. Available from: <https://doi.org/10.1007/BF02478259>.
- [7] LEIJNEN, S., van VEEN, F. The Neural Network Zoo. *Proceedings*. 2020, vol. 47, no. 1, 9. Available from: <https://doi.org/10.3390/proceedings2020047009>.
- [8] RABUNAL, J.R., DORADO, J. *Artificial Neural Networks in Real-Life Applications*. London: Idea Group Publishing, 2006.

- [9] ROSENBLATT, F. The Perceptron: A Probabilistic Model for Information Storage and Organization in the Brain. *Psychological Review*. 1958, vol. 65, no. 6, pp. 386-408. Available from: <https://doi.org/10.1037/h0042519>.
- [10] MINSKY, M.L., PAPERT, S.A. *Perceptrons: An Introduction to Computational Geometry*. Cambridge: The MIT Press, 1969.
- [11] BROOMHEAD, D.S., LOWE, D. *Radial Basis Functions, Multivariable Functional Interpolation and Adaptive Networks*. London: Malvern, Worcs.: Royals Signals & Radar Establishment, 1988.
- [12] BROOMHEAD, D.S., LOWE, D. Multivariable Functional Interpolation and Adaptive Networks. *Complex Systems*. 1988, vol. 2, 321-355.
- [13] SPECHT, D.F. A General Regression Neural Network. *IEEE Transactions on Neural Networks*. 1991, vol. 2, no. 6, pp. 568-576. Available from: <https://doi.org/10.1109/72.97934>.
- [14] OPĚLA, P., SCHINDLER, I., KAWULOK, P., KAWULOK, R., RUSZ, S., NAVRÁTIL, H., JURČA, R. Correlation among the Power Dissipation Efficiency, Flow Stress Course, and Activation Energy Evolution in Cr-Mo Low-Alloyed Steel. *Materials*. 2020, vol. 13, no. 16, 3480. Available from: <https://doi.org/10.3390/ma13163480>.
- [15] BEALE, M.H., HAGAN, M.T., DEMUTH, H.B. *Neural Network Toolbox™ 7: User's Guide*. [online]. 2010. [viewed: 2022-02-15]. Available from: <http://citeseerx.ist.psu.edu/viewdoc/download?doi=10.1.1.220.1640&rep=rep1&type=pdf>.
- [16] LEVENBERG, K. A Method for the Solution of Certain Non-Linear Problems in Least Squares. *Quarterly of Applied Mathematics*. 1944, vol. 2, no. 2, pp. 164-168. Available from: <https://doi.org/10.1090/qam/10666>.
- [17] MARQUARDT, D.W. An Algorithm for Least-Squares Estimation of Nonlinear Parameters. *Journal of the Society for Industrial and Applied Mathematics*. 1963, vol. 11, no. 2, pp. 431-441. Available from: <https://doi.org/10.1137/0111030>.
- [18] BAYES, T., PRICE, R. An Essay Towards Solving a Problem in the Doctrine of Chance. By the late Rev. Mr. Bayes, F. R. S communicated by Mr. Price, in a letter to John Canton, A. M. F. R. S. *Philosophical Transactions of the Royal Society of London*. 1763, vol. 53, pp. 370-418.
- [19] MACKEY, D.J.C. Bayesian Interpolation. *Neural computation*. 1992, vol. 4, no. 3, pp. 415-447. Available from: <https://doi.org/10.1162/neco.1992.4.3.415>.
- [20] RUMELHART, D.E., HINTON, G.E., WILLIAMS, R.J. Learning Internal Representations by Error Propagation. In: FELDMAN, J.A., HAYES, P.J., RUMELHART, D.E. (Eds). *Parallel Distributed Processing: Explorations in the Microstructure of Cognition*. Cambridge: The MIT Press, 1986, Volume 1: Foundations, chapter 8, pp. 318-362.
- [21] OPĚLA, P., SCHINDLER, I., KAWULOK, P., KAWULOK, R., RUSZ, S., NAVRÁTIL, H. On Various Multi-Layer Perceptron and Radial Basis Function Based Artificial Neural Networks in the Process of a Hot Flow Curve Description. *Journal of Materials Research and Technology*. 2021, vol. 14, pp. 1837-1847. Available from: <https://doi.org/10.1016/j.jmrt.2021.07.100>.
- [22] Euclid, of Alexandria, Adelard, of Bath, Campano, da Novara, Giovanni, M., Hypsicles, of Alexandria, Isidorus, of Miletus, Gherardo, da Cremona, Erhard, R., Adams, J.C. *Preclarissimus liber elementorum Euclidis perspicacissimi in artem geometrie incipit Qua foelicissime [The Most Famous Book of Euclid's Elementary Observations in the Art of Geometry Which Begins 'Qua foelicissime' (Euclid, ca. 300 A.C.N.)]*. Venice: Erhardus Ratdolt Augustensis impressor solertissimus, 1482.
- [23] GAUSS, J.C.F. *Theoria motus corporum coelestium in sectionibus conicis solem ambientium [Theory of the Motion of the Heavenly Bodies Moving about the Sun in Conic Sections]*. Hamburg: Friedrich Perthes and I. H. Besser, 1809.
- [24] LEGENDRE, A.M. *Nouvelles méthodes pour la détermination des orbites des comètes [New Methods for the Determination of the Orbits of Comets]*. Mesnil-sur-l'Estrée: Firmin Didot, 1805.